

A Bidirectional Soft Diode for Artificial Systems

Artur Davletshin, Thomas C. Underwood, and Wen Song*

Artificial material systems that seek to mimic the basic processes of life must perform multiple complex functions, including responsiveness, motion, and metabolism. Networks of programmable materials offer a pathway toward achieving these functions by altering local chemical, physical, and structural properties to enable control. The ability to perform multiple complex functions in a single soft elastomeric material system is demonstrated by reconfiguring, in situ, passive bistable fluidic diodes that are inspired by mammalian venous valves. It is shown how pneumo-mechanical programmability allows these silicone elastomer diode assemblies to accomplish, without rearranging the fluidic circuit, multiple functions, including pumping (motion), energy storage/discharge (metabolism), logic operations (response), and signal filtering/rectification. The ability to achieve multiple functions through in situ programming may lead to the development of efficient artificial systems capable of complex functions in compact, remote applications.

1. Introduction

The ability for simple nucleotides to assemble into complex, multifunctional genetic instructions offers inspiration for designing new classes of functional materials that aim to mimic life.^[1] Current approaches to achieve motion, responsiveness, and metabolism leverage programmable materials that change their form, function, or state on demand.^[2] These materials use a combination of physical and chemical properties to sense their environment and regulate a desired behavior (i.e., exert a form of control).^[3] Currently, reconfigurable matter (i.e., components) carry out predefined actions (e.g., shape change,^[4–7] self-assembly,^[3,8,9] pattern formation^[10–12]) to perform a specialized function. Mimicry of complex life (e.g., integrated artificial responsiveness, motion, and metabolism), therefore, relies on

collaboration between many such specialized components—integrating the multitudinous components is a complex task that leads to system inefficiency (i.e., high energy expenditure, lack of compactness and modularity) and/or simplicity in function. To enable complex artificial life, a new design strategy is required where networks of simple, passive components can be assembled, reconfigured, and programmed on-demand to perform multiple functions.

Here, we demonstrate a set of multifunctional and programmable behaviors that are enabled by network assemblies of simple, passive bidirectional fluidic diodes (i.e., one-way valves) in which flow is regulated, without external energy input, in two opposing orientations. The passive characteristic of the soft diode component


maximizes the energy efficiency of the system (i.e., no parasitic loads), while first-of-a-kind programmable bidirectionality (i.e., switchability between two distinct states, **Figure 1**) enables multifunction, simplicity, and modularity in design. The basic function of the fluidic diode in regulating the direction of flow, coupled with its programmable bistability and modularity, is leveraged here to enable the efficient design of multifunctioning material systems. For example, reprogramming the orientation of two fluidic diodes assembled in series enables the basic functions of pumping (both in state 1 or state 2, fluid displacement or motion, **Figure 2**) and energy storage and release (state 1 and state 2, metabolism, **Figure 3**), while state-switching of a diode pair assembled in parallel enables the elementary logic operations AND (state 1) and OR (state 2) to mimic “thinking” (**Figure 4A**). Similarly, reconfiguring a single diode enables both filtering and rectification of fluid flow (i.e., information transfer, **Figure 4B**). The functions enabled by programming the simple, passive diode components minimize operational energy expenditures in soft artificial systems to achieve complex behavior with efficiency, compactness, and modularity to mimic life.

While the idea of programmable multifunctioning systems has been demonstrated previously in electronic circuits (i.e., field programmable gate arrays) where hardware (i.e., individual logic blocks) can be reconfigured to program different functions on-demand, implementation in soft artificial systems is lacking. The continuous deformation afforded by soft (elastomeric) materials is well-suited to perform the range of complex functions for artificial systems to mimic life. So far, soft matter integrated with responsive elements (e.g., light-sensitive polymers,^[6] hydrogels,^[13–15] etc.) have been limited to achieving single specialized functions (e.g., self-folding,^[16,17]

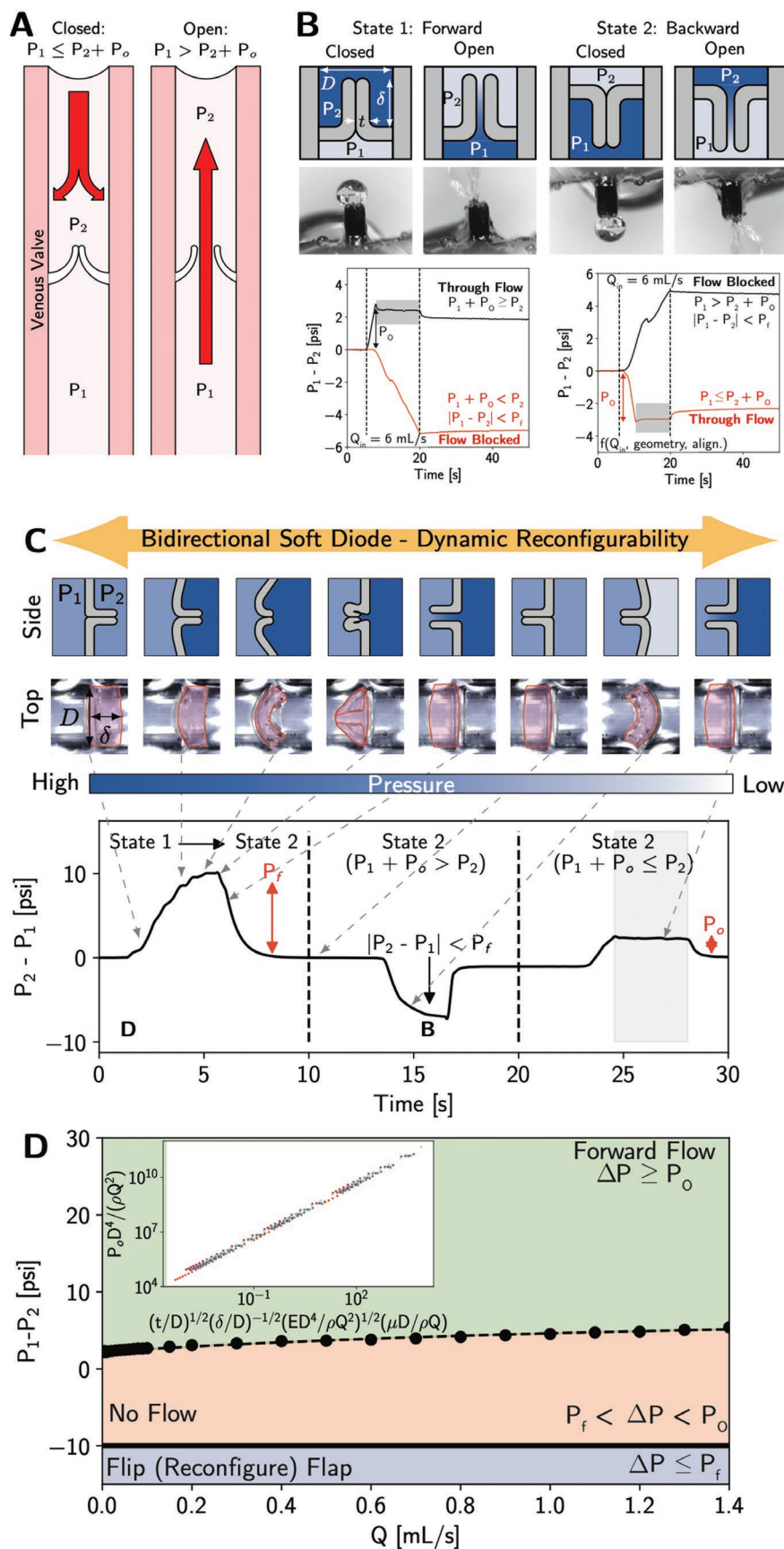
A. Davletshin, W. Song
Center for Subsurface Energy and the Environment
University of Texas at Austin
Austin, TX 78712-1585, USA
E-mail: wensong@utexas.edu

T. C. Underwood
Department of Aerospace Engineering and Engineering Mechanics
University of Texas at Austin
Austin, TX 78712-1585, USA

T. C. Underwood, W. Song
Texas Materials Institute
University of Texas at Austin
Austin, TX 78712-1585, USA

 The ORCID identification number(s) for the author(s) of this article can be found under <https://doi.org/10.1002/adfm.202200658>.

DOI: 10.1002/adfm.202200658



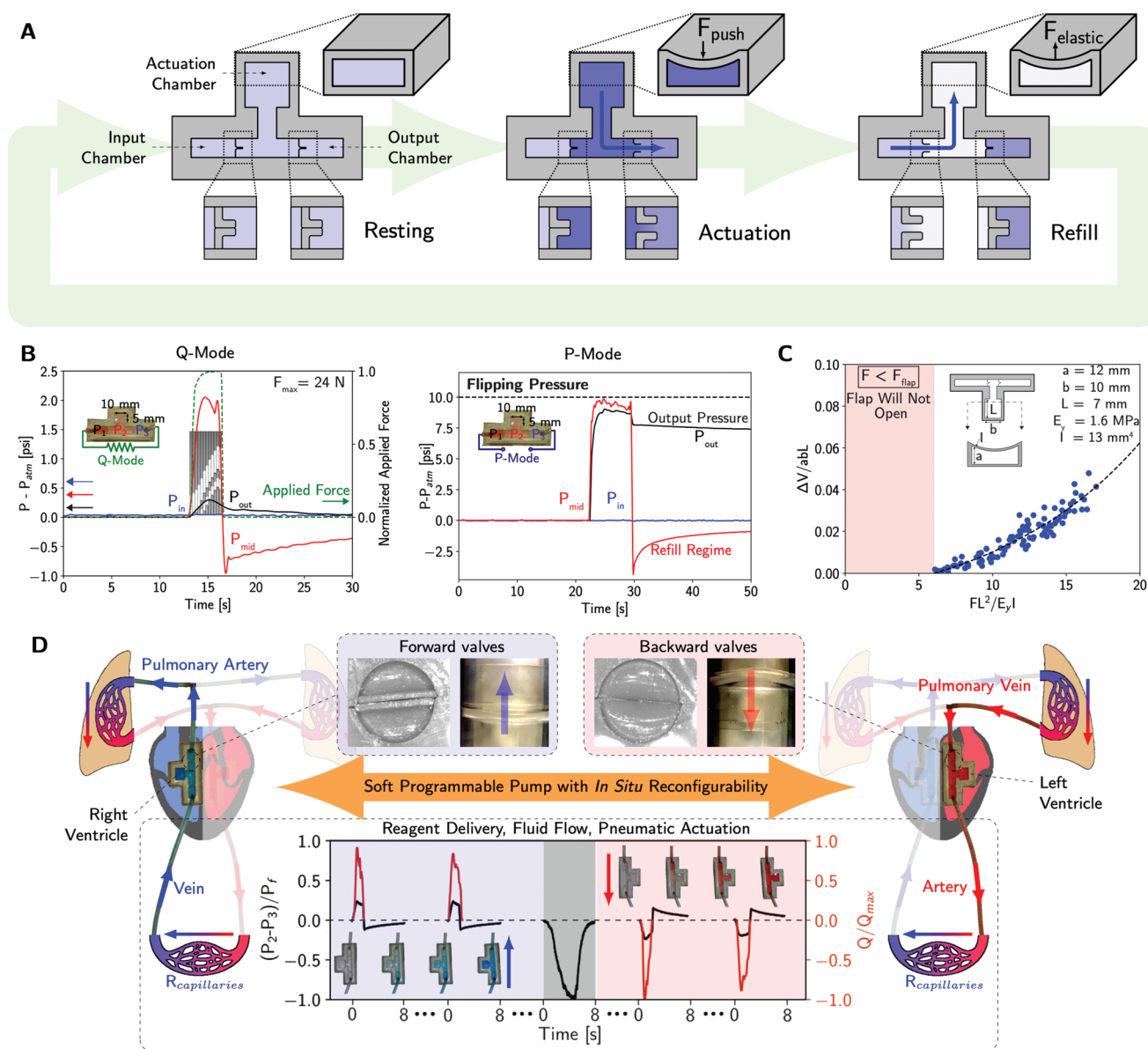


Figure 2. A programmable soft pump using two reconfigurable diodes in series. A) Schematic actuation of the soft pump, where compression of the actuation chamber (actuation) pressurizes the enclosed fluid to force flow out of the downstream valve and close the upstream valve, and release of the actuation chamber (refill) draws a vacuum within the chamber to allow flow in from the upstream valve and closes the downstream valve. B) Two modes of operation, rate (Q-mode) and pressure (P-mode) control, are possible depending on the connected fluidic load (i.e., resistance). C) Dimensionless characterization of the displacement fluid volume, ΔV , as a function of the actuation chamber geometry (a, b, L), elasticity, E_y , and applied force, F . D) A reconfigured pump operating in two directions, like the left and right sides of mammalian hearts. Pressure signals resulting from pump actuation resemble those from electrocardiograms of the heart. Pressure pulses ($P_2 - P_3$) are normalized to the flipping pressure (P_f) required to reverse the direction of the valves, and resulting flow rates are normalized to the maximum flow rates measured Q_{max} .

Figure 1. A programmable soft diode that enables multifunctional design. A) Design of the diode is inspired by venous valves in the human vasculature, where tissue leaflets form one-way valves to prevent backflow of blood. B) The diode is stable in two states and rectifies flow in a similar fashion as venous valves in each state. C) Unlike venous valves, the diode is reconfigurable between the two stable states by imposing a pressure gradient in the direction opposing the valve leaflets (P_f). Stability in each state allows the diode to retain its configuration without an external supply of energy. D) Three regimes are defined for information transfer through the bidirectional valve: forward flow (green, pressure signal is transmitted), no flow (orange, pressure signal is obstructed), and reconfiguration (blue) where the valve leaflet direction is reversed. Nondimensionalization of the open pressures (P_o) show that the modulatory characteristics of the valve depend on the leaflet dimensions (t, δ), channel geometry (D), fluid properties (Q, ρ, μ), and material elasticity (E_y) of the device (inset, each data point represents at least 3 trials).

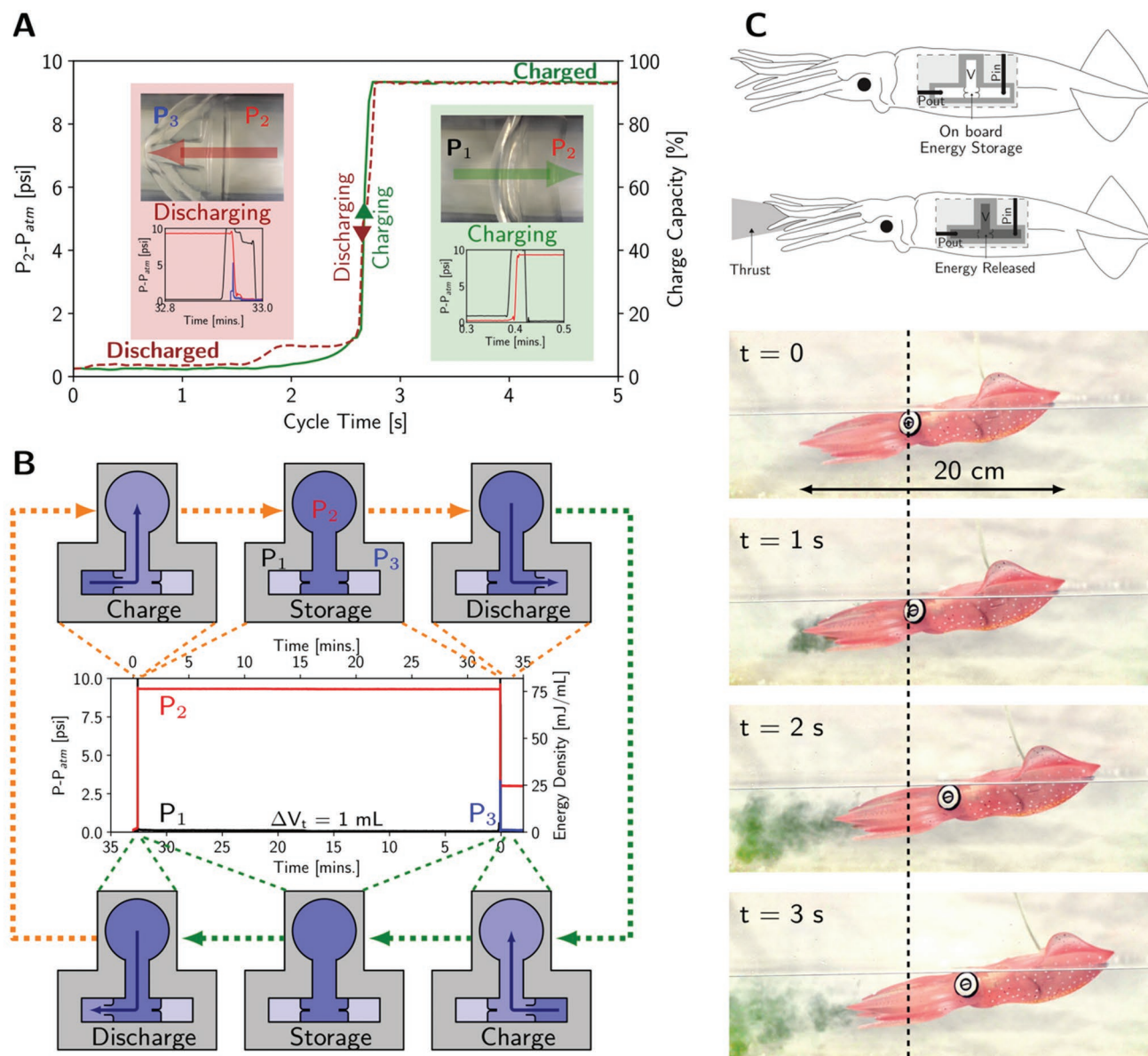


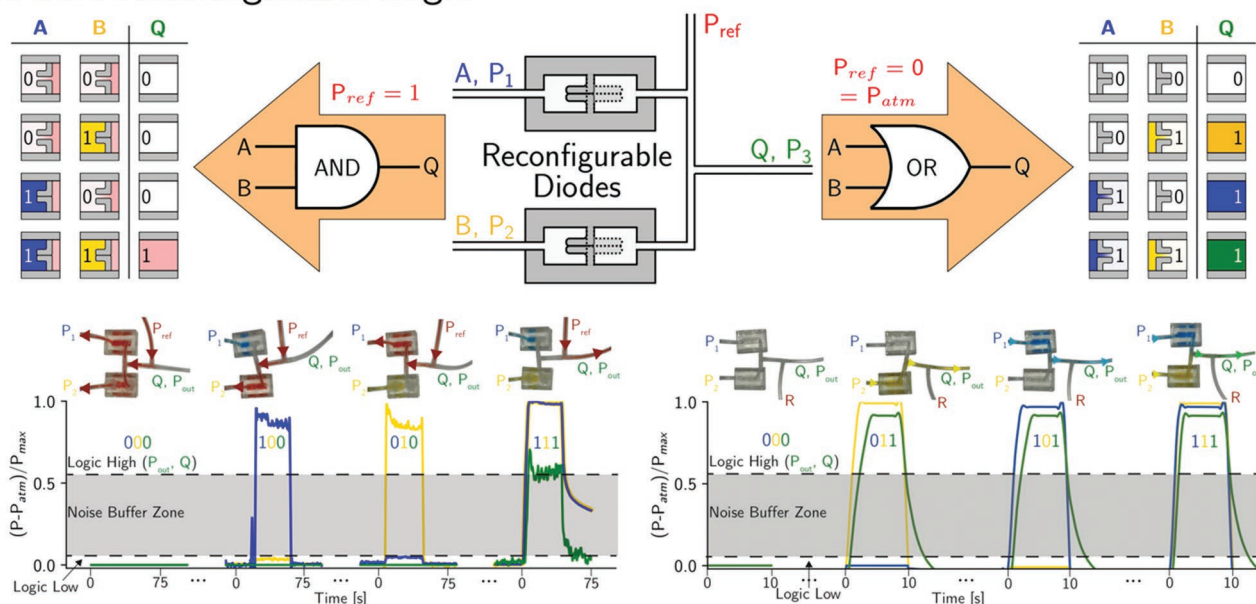
Figure 3. Energy storage using the two diodes in series. A) Charge/discharge cycles leverage the reconfigurability of the diodes. B) Passive stability in each state allows charging and stable energy storage (P - V work). Energy is discharged by reconfiguring the output diode. C) Stored energy is discharged in an artificial squid, mimicking jet propulsion of cephalopods in nature.

change shape,^[18,19] etc.). Examples of specialized soft systems controlled by external electromagnetic forces and applied pressures include stretchable pumps,^[20–22] artificial muscles,^[23–28] fluidic computation components (e.g., ring oscillator,^[29] logic gates,^[30] circuit components^[31–33]), and material actuation,^[34,35] but lack multifunctioning capability. A soft matter component that can be used to implement multiple functions (e.g., actuate, compute, and store energy) by leveraging mechanical programmability is still missing and is necessary to enable efficient design and autonomous complexity in future artificial material systems.

2. Results and Discussion

To enable multifunction in soft matter, we develop an elastomeric bidirectional fluidic diode that is programmable to regulate fluid flow passively in two orientations (i.e., each orientation acts as a one-way valve that operates without external energy input, Figure 1). Importantly, our soft fluidic diodes are distinguished by a pair of elastomer leaflets whose states switch dynamically between two distinct states (state 1 and state 2, Figure 1B) in response to pressure signals. This reconfigurability enables programmable changes in system function

A Soft Reconfigurable Logic



B Soft Analog Circuitry

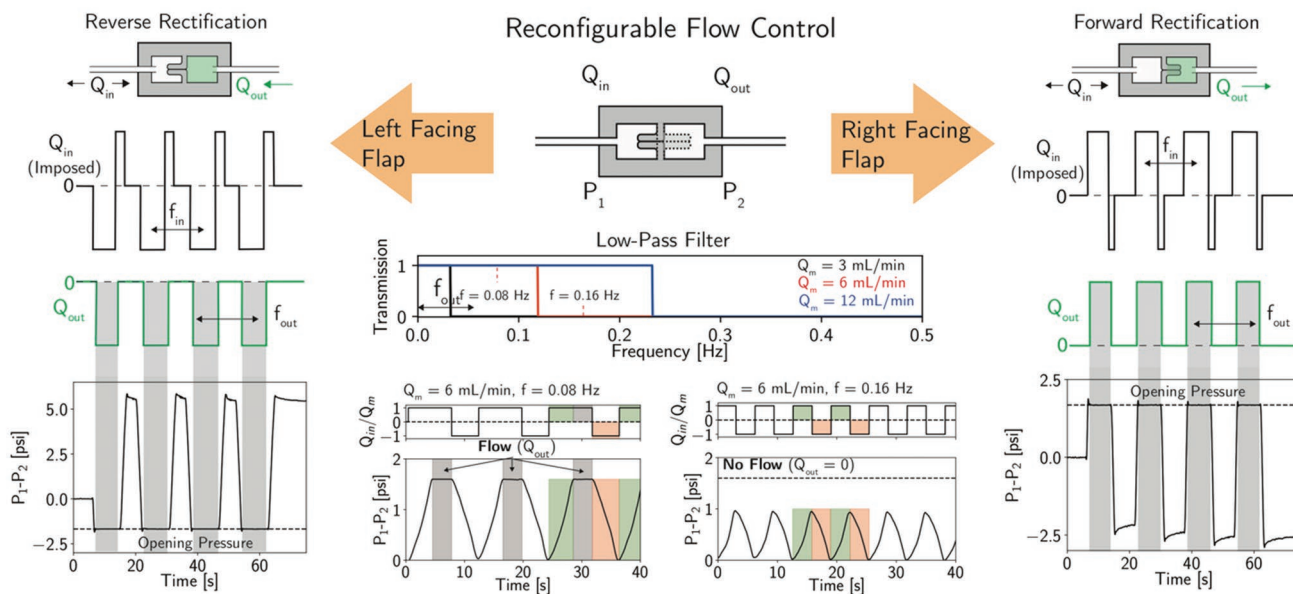


Figure 4. Reconfigurable digital logic using two soft diodes in parallel. A) Combinations of diodes can be connected to form elementary digital logic gates (AND, OR) and be reconfigured on demand by changing the orientation of the leaflets. B) The diode can also rectify and filter analog signals (e.g., pressure and flow rates) depending on the orientation and geometry of the leaflets.

without rearranging the fluidic circuit. Here, multifunction results from reconfiguring the state of individual diodes that are assembled in networks by modulating the direction of information transfer (i.e., flow). The elastomeric diodes (PDMS, Dragon Skin 10, Dragon Skin 30) comprise a flow channel (diameter $D \approx 4\text{--}8$ mm) embedded with a pair of valve leaflets (thickness $t \approx 400\text{--}800$ μm , overlaps $\delta \approx 1$ to 3 mm, Figure 1) that control the magnitude (zero or positive) and direction of flow (forward and backward). The valve leaflets are thin

membrane sheets (rectangular protrusions larger than half the cross-section of the channel) that when compressed together, deform into two portions: one that lies along the cross-section of the channel and obstructs flow (i.e., cross-sectional portion), and another that lies along the axis of the channel (i.e., an overlapped region with overlap length δ) that rectifies flow, defines diode states, and enables passive bistable memory (i.e., maintaining the state by elastically deforming within the geometric constraints of the channel). The form and structure of the diode

is inspired by venous valves where blood flow is regulated in a single direction to prevent backflow of blood due to gravity^[36,37] (Figure 1A), however a key distinction is in the bistability of the diode (Figure 1B,C). Whereas venous valves, and likewise duckbill valves that were inspired by valves in the vasculature, consist of a single continuous mass, construction of the fluidic diode using two separate leaflets allows for reversals in the direction of the overlaps and thus bidirectionality.

Material memory (i.e., stable configuration of the leaflets due to elastic deformation and geometric constraints of the channel) in the diode enables passive flow modulation without external energy input. The function of the diode relies on a compressive stress that deforms the valve leaflets to rectify flow in the channel passively (Figure 1). For a given state (Figure 1B), information transfer is controlled by the alignment and magnitude of the imposed pressure gradient, $\Delta P = P_1 - P_2$, relative to the orientation (direction) of the leaflet overlaps and the force required to overcome material compression from the geometric constraints imposed (i.e., characteristic opening pressure of the diode, P_o). For instance, ΔP applied in the direction opposing the orientation of the overlap prevents information transfer. For ΔP applied in the same direction of the overlap, two different regimes of information transfer are possible: no flow where the imposed pressure gradient is less than the characteristic opening pressure of the diode ($\Delta P < P_o$), and flow otherwise ($\Delta P \geq P_o$, Movies S1–S3, Supporting Information).

To transform between the two different states (Figure 1C, Movie S4), we impose a pressure gradient in the direction opposing the leaflet overlap. As pressure is applied, the normal force exerted onto the valve leaflets closes the overlaps onto one another and deforms the remainder of the leaflets (i.e., the cross-sectional portion that obstructs flow). Keeping the overlaps compressed allows further pressure buildup to elastically deform the thin leaflets. Deforming the cross-sectional portion of the valve leaflets out of its original resting position expands the volume and surface area of the pressurized chamber, and therefore reduces the contact area between the overlapping portion of the two leaflets. The process continues until the overlapping area is reduced to zero (i.e., $-\Delta P = P_f$, flipping pressure), at which point momentum and material elasticity flip (i.e., reconfigure) the overlaps to its alternate stable orientation (i.e., state 2, Figure 1B).

For sufficiently large channel diameter to leaflet length and thickness ratios (D/δ , D/t), the device is approximated as a two-dimensional system. Edge effects (i.e., interactions between the leaflets and the wall channel), however, remain important as the edges of the leaflets are forced into contact with the channel walls because of the compressive forces applied by the channel geometry. Interactions between the edges of the leaflets and the channel walls (i.e., surface adhesion) result in local resistances to slip between the surfaces in contact. During opening of the valve, the edges of the leaflet overlaps experience additional forcing into the channel walls and are therefore pinned to the channel wall (i.e., act as a fixed boundary condition). During reversal of leaflet direction (flipping), however, the edges of the leaflet overlaps are pulled away from the channel walls by the material strength of the polymer. Edges of the cross-sectional portions of the leaflets are pinned at the wall, and deformation

due to an opposing pressure gradient during flipping causes a curved leaflet surface (Figure 2B).

Reliability in the reversal characteristics of the bidirectional valve is required to program soft artificial materials to mimic life processes. The characteristics that control reversal between the two states is dependent upon the valve geometry (i.e., leaflet thickness and overlap, channel diameter), material elasticity, and the pressure pulse applied. For the valve in Figure 1C (PDMS, thickness $t \approx 600 \mu\text{m}$, overlap $\delta \approx 2 \text{ mm}$, channel diameter $D \approx 6 \text{ mm}$, $P_{\text{flip}} \approx 10.585 \text{ psi}$), the valve maintained a constant flipping pressure of $P_{\text{flip}} = 10.585 \pm 0.035 \text{ psi}$ over the course of ≈ 330 reversals (Figure S3, Supporting Information). Each state reversal occurred over $\approx 0.29 \text{ s}$ when using a pressure pulse generated by a constant flow rate of 1 mL s^{-1} . The reliability and rapid rate of state switching leads to advantages in using the bidirectional diode in “thinking,” “motion,” and “metabolism” in soft material systems, where the rate of “processing information” is limited by the rate at which data signals (i.e., pressure pulses) are supplied.

To enable multifunction behavior at an array of scales, we tune the characteristics of the device by controlling its opening and flipping pressures (P_o , P_f , Figure 1D). We perform dimensional analysis (see Supporting Information) on the opening pressure of a series of bidirectional soft valves with varying dimensions and elasticity to show that the flow modulation characteristics of the diodes can be described by four dimensionless groups comprising the leaflet geometry (thickness, t , and length of the overlap, δ), channel diameter, D , material elasticity, E_p , and hydrodynamic properties of the working fluid (flow rate, Q , fluid viscosity, μ , density, ρ) (Figure 1D, inset, and Figure S4, Supporting Information). The tunability of the diodes, in addition to their bistability and programmable reconfigurability, offers a new method to modulate information transfer in different directions and leads to the construction of artificial systems capable of complex multifunctional behavior.

We demonstrate the multifunction performance of assembled fluidic diode networks using series and parallel fluid circuits. In series, two identical diodes (e.g., same geometries and elasticity) yield a soft reconfigurable pump (Figure 2) and a soft energy storage system (Figure 3) depending on the orientation (i.e., state) of the diodes. When both diodes are oriented in the same direction, the circuit becomes a mechanical soft pump where the two diodes isolate three separate chambers (Figure 2A): an input chamber that supplies fluids (i.e., input information, P_{in}) for refilling the pump, an actuation chamber that generates pressure to displace fluids (P_{mid}), and an output chamber that delivers the displaced fluid (i.e., transmitted information, P_{out}) to a target. The pump described here operates similarly to one side of a mammalian heart: the ventricle (i.e., actuation chamber) is compressed to expel blood into the artery (i.e., output chamber), and relaxes to fill with blood from the atrium (i.e., input chamber, Figure 2A,D, Movie S5, Supporting Information). Here, external forcing (i.e., mechanical compression) on the soft actuation chamber forces the chamber walls to deform, and the chamber contracts volumetrically (Figure 2A,B, actuation). The reduced volume corresponds to a positive pressure buildup that forces the input diode to close ($P_{\text{mid}} > P_{\text{in}}$) and the output diode to open and displace the fluid ($P_{\text{mid}} > P_{\text{out}}$). The rate of fluid displacement

(i.e., flow rate) depends on the change in volume induced and the rate of actuation. To refill the pump, the external force is removed so that the elastic actuation chamber can restore its original shape and volume (Figure 2A,B, refill). The expansion in volume causes pressure to decline in the actuation chamber, imposing a positive pressure differential across the input diode (open, $P_{\text{mid}} < P_{\text{in}}$) and a negative pressure differential across the output diode (closed, $P_{\text{mid}} < P_{\text{out}}$) to allow fluids from the input chamber to fill the actuation chamber. Based on the fluidic load (i.e., resistance) of the circuit, this soft diode pump can be used to create either positive volumetric displacements (Q-mode, closed circuit) or generate a fixed output pressure (P-mode, open circuit, Figure 2B). The displaced volume scales with the force applied to the actuation chamber, F , and the characteristics of the diodes (elasticity, geometry, Figure 2C). It is possible to pump fluids in the reverse direction, as with the other side of the mammalian heart, by reprogramming the pump in situ. We demonstrate the bi-directional pump by applying a local pressure pulse to flip the orientation of both diodes (Figure 2D). In doing so, the pump switches between operating as the “right” and “left” sides of the heart.

A second function of the two diodes in series allows for cyclic energy storage and discharge (Figure 3). When the two diodes are oriented in opposing directions (i.e., the outlets of the diodes face each other), fluid (i.e., energy) injection through either diode causes a pressure buildup in the middle (i.e., storage) chamber ($P_1 < P_2 > P_3$) where the fluids cannot be released as in the pump. The increase in pressure in the storage chamber is stored pressure–volume work (P – V , Figure 3A,B). Energy storage is possible so long as the pressure differential across the valve is less than its characteristic flipping pressure ($|P_{1,3} - P_2| < P_f$). For the diodes described in Figure 1, there was no loss in stored energy over an \approx hour period ($P_2 = \text{const}$, Figure 3B). To discharge the stored energy, the diode that is connected to a load is simply reversed. In a way, this system becomes a rechargeable soft energy storage system, where charge/discharge cycles are marked by programming the diodes in opposing (charge) or the same (discharge) orientations (Figure 3B). The energy stored and discharged from such a system and the longevity of the “battery” depends on the storage cavity (volume and expansivity, Supporting Information), compressibility of the working fluid, diode flipping pressure, and elastic material properties, all of which are design parameters that can be tuned. For example, we achieve energy charge and discharge cycles of $\approx 76 \text{ mJ cycle}^{-1}$ by injecting/ejecting $\approx 1 \text{ mL}$ of water through the pair of PDMS diodes described in Figure 1 (see Supporting Information for calculations). Importantly, once assembled, the cycle health (i.e., number of charge/discharge cycles before losses in cycle efficiency) of the system depends only on the ability of the elastomeric material to withstand elastic deterioration. Recall, importantly, that the pressure required to reverse the direction of the diode remains constant $P_{\text{flip}} \approx 10.585 \pm 0.035 \text{ psi}$ over 330 state reversals (Figure S3, Supporting Information).

The efficiency of the present energy storage and discharge cycle is $\eta = W_{\text{net}}/E_{\text{in}}$, where the net work out of the system is the energy stored less the energy required to reverse the valve ($W_{\text{net}} = E_{\text{stored}} - E_{\text{flip}}$), and the energy input into the system is the sum of the energy stored, the energy required to flip the valve, and

the energy required to open the valve ($E_{\text{in}} = E_{\text{stored}} + E_{\text{flip}} + E_{\text{open}}$). If we neglect the energy that is associated with opening the valve here, given that it is much smaller than the energy required to flip the valve and the energy stored, then the energy efficiency is $\eta \approx (E_{\text{stored}} - E_{\text{flip}})/(E_{\text{stored}} + E_{\text{flip}})$ and suggests that minimizing the flipping energy allows the storage efficiency to approach 100%. Following this analysis, approaches to maximize the energy efficiency is to (a) maximize the E_{stored} by maximizing the volume of the storage vessel, or (b) minimize the E_{flip} by increasing the channel diameter, decreasing the length and thickness of the valve leaflets, and using an elastomer with lower stiffness. We note, however, that the energy stored is the PV work of the system, and minimizing the flipping energy reduces the pressure that the storage vessel can withhold and thus reduces the amount of energy stored (i.e., tradeoff between energy stored and storage efficiency).

To demonstrate the utility of storing and dispensing energy using reconfigurable diode components in actuating soft artificial systems (i.e., to mimic metabolic processes), we emulate the jet propulsion of cephalopods (Figure 3C, Movie S6, Supporting Information). Cephalopods can swim at up to $\approx 2 \text{ m s}^{-1}$ by expelling, through its siphon, a pressurized jet of water that is stored in its mantle cavity.^[38] Here, we embed our soft energy storage circuit in the mantle of an artificial squid. We rely on the material memory and bidirectionality of the diode to carry out jet propulsion (i.e., energy discharge) in the artificial squid instead of muscle contractions. Using a diode-pair with $\approx 76 \text{ mJ}$ of stored energy, we achieved peak jet velocities of $\approx 1 \text{ m s}^{-1}$ by ejecting $\approx 1 \text{ mL}$ of water at a discharge rate of 0.35 W (volumetric energy density $\approx 60 \text{ kJ m}^{-3}$, Figures S4 and S5, Movie S7, Supporting Information). While the energy density achieved here is ≈ 2 orders of magnitude less than that of other energy storage mechanisms such as pumped hydropower ($\approx 1800\text{--}5400 \text{ kJ m}^{-3}$) ref. [39], the key advantage offered here is in the modular-, soft-, and liquid-compatibility that enables interfacing with extreme environments (e.g., deep ocean, human–machine interface, etc.).

Beyond diode circuits in series, parallel networks of the reconfigurable components allow the field implementation (i.e., after assembly) of programmable computing. Logic operations performed by reconfigurable elementary logic gates (AND and OR) are possible by arranging two identical diodes in parallel (Figure 4A). Each diode is connected to an input (A, B) on one side, and connected to the output (Q) on the other. A reference pressure is connected to the output to moderate the signal. Pressure is the logic variable that is 1 if the pressure differential exceeds the characteristic opening pressure (i.e., if fluid flows through) and is 0 otherwise. The OR operation is performed when both diodes are oriented toward the output and the reference pressure is atmospheric. In this configuration, if either or both of the input signals are 1 (i.e., input to diode A and/or B has $\Delta P > P_0$), then the input signal will be transmitted to the output ($Q = 1$, $P_Q > P_0$). Conversely, if both input signals are 0 (i.e., input to both diode A and B are such that $\Delta P < P_0$), then no fluid signal is transmitted across the diodes and the output remains $Q = 0$ ($P_Q < P_0$). Similarly, an AND gate is programmed by reconfiguring the diodes of the OR gate to face the input and by imposing a logic high (i.e., 1) to the reference pressure. In this case, the signal from P_{ref} is dissipated through the diodes

if any of the input signals are 0 (i.e., $\Delta P < P_0$), and therefore the output remains $Q = 0$. In the case where both input signals are 1 (i.e., $\Delta P > P_0$), the high-pressure signal from P_{ref} can no longer be dissipated, and the output becomes $Q = 1$. The ability to reprogram the function of existing logic gates (i.e., switching between AND and OR functions) allows for in situ programming of logic gates and the imitation of “thinking” in artificial material systems to mimic life. The reliability of the pneumatic logic gates here is highlighted by the consistent flipping characteristics of the device (constant $P_{\text{flip}} \approx 10.585 \pm 0.035$ psi over ≈ 330 reversals).

Bidirectional stability in the soft diodes offers many opportunities toward achieving artificial life. The combination of signal filtering, rectification, and reconfigurability (Figure 4B), allows for individual soft diodes to control and process information in environments that are not amenable to conventional electronics (e.g., human–machine interface, deep ocean environments, etc.). Each diode here is able to rectify information (pressure) signals by allowing unidirectional communication. Filtering of high-frequency noise (i.e., rapid pressure signals) is possible using the diodes described by either preventing flow in the case where the pressure gradient opposes the direction of the valve leaflets, or attenuating flow in the case where the pressure applied along the direction of the leaflets is small ($\Delta P < P_0$). Key advantages of the bidirectional diode here are that it is: (i) passive and does not require any external energy input to maintain its state or function, and (ii) bistable and allows programming after assembling the circuit, much like field-programmable gate arrays (FPGAs) in electronic circuits.

3. Conclusion

The demonstrations here show how soft, reconfigurable components can enable multifunctional behavior by allowing field programmability after assembly. Combining unique elastomeric states with passive flow control allows diodes to programmably switch between actuation and energy storage or computational operations depending on the state of the diode components. The modular reconfigurability and passive nature of the soft diode can lead to new classes of programmable materials for improved control and complex functions to achieve artificial life at the human scale. The advantage of using the valves here for applications such as propulsion, motion, and logic lies in their soft and liquid-compatible nature. For example, in extreme environments such as the deep sea where conventional electronics struggle (water-compatibility, vessel design to withstand high pressures), a soft, fluid-analog actuator provides the ability to leverage its surrounding environment for locomotion and sensing (e.g., valves are sensitive to pressure differentials and thus can be used to measure the depth of the device). Similarly, in systems that must be sensitive to forces (e.g., human–machine interface), a pneumatic set of logic gates such as those described here enables “sensing,” which has been difficult to achieve to date.

4. Experimental Section

Materials: Soft diodes were manufactured using a combination of silicone elastomers and Tygon tubing. Different silicone elastomers were

used to quantify the effect of material elasticity (i.e., Young’s modulus) on the properties of the diode. Each silicone elastomer was purchased commercially and used as received. Polydimethylsiloxane (PDMS) was purchased as a 0.5 kg Sylgard 184 kit from Ellsworth Adhesives. Dragonskin 10 (Medium) and 30 were purchased from Smooth-On, Inc. The elastomers were prepared following industrial protocols (see fabrication section for specifics). Tygon tubing with a 1/16” (0.16 cm) ID and 1/8” (0.32 cm) OD was purchased from McMaster-Carr.

Water soluble dyes were used to visualize fluid flow between diodes. A combination of Brilliant Blue FCF, Allura Red AC, Fast Green FCF, and Tartrazine were purchased in a concentrated aqueous form (20 mL) by Aldon and delivered through VWR. Between 50–500 μL of each dye was added to 20 mL of water to adjust the contrast of each solution.

Soft Diode Fabrication: The diodes were fabricated using a custom soft lithographic procedure (Figure S1, Supporting Information). The procedure was optimized to enable reproducible and simple diode fabrication that spans multiple scales (i.e., channel diameter, leaflet thickness, etc.). Assembly took place over four distinct steps to mold, cure, and bond the diode using elastomeric materials. It demonstrates that this procedure enables extracting (without tearing) the valve leaflets with widths < 400 μm and aspect ratios (i.e., channel diameter/leaflet width) < 0.1 .

The soft diodes were fabricated in stages by casting elastomers on 3D printed molds (Figure S1, Supporting Information). Each mold was printed by a Stratasys Objet30 Polyjet 3D Printer using Vero Family Acrylic materials. The printer has a spatial resolution of ≈ 100 μm that is smaller than the leaflet dimensions considered in this work. Following printing, each mold was conditioned at 60 $^{\circ}\text{C}$ for 72 h to ensure that elastomers did not stick to the mold. Molds that were not conditioned resulted in torn leaflets during extraction. Each mold was designed in CAD to cast half of a diode with a circular cross-section (i.e., a longitudinal slice). A rectangular slot was extruded and removed from the channel at the center of each mold, and the slot was filled with elastomer to create a leaflet. Each leaflet was longer than the radius of the channel that it was cast in to create leaflet overlaps that are required for flow rectification. Diode geometries characterized in the work include channel diameters between 4 and 8 mm, leaflet thicknesses between 400 and 800 μm , and leaflet overlaps between 1 and 3 mm.

Elastomers were used as received and prepared according to manufacturer specification. This process involved mixing a base and curing agent thoroughly for 30 min, degassing under vacuum (≈ 100 Torr) for another 30 min, and pouring it in the mold. Sylgard 184 (PDMS) was used with a 10:1 ratio of base to curing agent and was cured in the mold at 60 $^{\circ}\text{C}$ for 6 h. Dragon Skin 10 and 30 were used with a 1:1 mixing ratio and cured in the mold at room temperature for 16 h (Figure S1, step 1, Supporting Information). Following curing, each elastomeric half-diode was extracted from the mold (Figure S1, step 2, Supporting Information), and holes were struck to enable flow. The mold was reused without additional treatment.

Cured components were next assembled into soft diodes. The outer edges of each half-diode were painted with a thin layer of uncured elastomer (of the same composition) so that when brought together and heated, the two half-diodes are bonded permanently (Figure S1, step 3, Supporting Information). Importantly, no elastomer was added to the leaflets to ensure that fluid flow is possible through the diode. To deform the leaflets as required in the valve, the half-diodes were subjected to a compressive force during curing (60 $^{\circ}\text{C}$ for 6 h). A binder clamp (≈ 4 N) was used to apply the external compression. Once cured, the diodes feature a pair of leaflets that are not bonded but remain in contact under a constant state of compressive deformation to allow for flow rectification and bistable reconfigurability.

Soft Pump and Energy Storage Fabrication: Soft pumps and energy storage devices were manufactured using the same procedure as described for the soft diode. Molds were designed that incorporate two soft diode leaflets using the same Objet30 Polyjet printer. A region in between the two leaflets was added to store energy and actuate the pump. The volume of this region (thickness a , length L , width b) was varied from 0.84 to >100 mL to store different amounts of energy. The wall thickness of this region was chosen to be 2.5 mm to allow deflection and the pumping of fluids by applying an external force. The same

elastomers, treatment, conditioning, and extraction process was used as with single diodes. Conditioning of the mold enabled the simultaneous extraction of many (> 1) leaflets without tearing.

Pressure Measurements: Pressure was recorded using a combination of an Arduino Uno microcontroller and multiple Honeywell SSCDRNT1.6BAAA3 pressure transducers (Figure S4, Supporting Information). Each pressure transducer was a piezoresistive silicon sensor offering a ratiometric analog output for reading pressure up to a full-scale value of 1.6 bar. Each transducer had an internal vacuum reference, a hose connector for 1/16" ID Tygon tubing, and had an output voltage proportional to the absolute pressure of the fluid stream. The linear factory calibration was independently confirmed by applying known fluid pressures and recording the output voltage.

Output voltages for the pressure transducers were recorded using the ADC on an Arduino Uno. The ADC featured a 10-bit (0–1023) resolution for measuring signals. A script was written for the microcontroller to sample up to 3 pressure transducers (i.e., for the input, middle, and output volumes of the pump) at rates between 10–100 Hz. This data was recorded using pySerial on a computer and saved in csv format.

Visual Data Collection and Processing: Image and video data of the diodes were collected using a USB microscope (Dino-Lite Edge AM 4115T-JV, Dino-Lite US, Torrance, CA) at magnifications of 10 to 220. Video data was recorded at 8 fps. The opening and closing of the diodes in each state was recorded by imaging the valve leaflets in the axial direction. Diode reconfiguration between the two states was recorded from the top of the diode to observe the deformation of the leaflets. System-level functions (e.g., pumping, energy storage, and logic) and their reprogramming were recorded similarly. Video of energy release was capturing using a Phantom V12 camera at 1280 × 800 resolution at 160 fps.

Quantification of the visual data was performed through image processing. Flow rates from the diode pump were quantified by measuring the displacement of water–air interfaces between adjacent image frames.

Force Characterization: Force measurements were performed using a combination of a precision balance and a force sensitive resistor (FSR). A Mettler-Toledo ME-T precision balance with a 3.2 kg capacity and a 0.01 g resolution was used to quantify the range of forces that were applied to actuate the pump. An Ohmite FSR01 resistor was configured in a voltage divider network to quantify the timescales over which the force was applied. The FSR featured a variable resistance that depended on the applied load, $R_{FSR}(F)$. Timescales were measured by recording the output voltage of the voltage divider circuit, $V_{out} = V_s/[1 + R_{FSR}/R_M]$, using an Arduino Uno microcontroller with a sample rate up to 500 Hz. The measuring resistor, R_M , was varied between 3 and 100 k Ω to control the saturation force of the voltage divider. A constant supply voltage, V_s , of 5 V was used for analysis.

A soft pump was characterized by placing it on a precision balance with an FSR affixed on top. The balance was zeroed, and the force of mechanical actuations were recorded by logging the balance and recording the output voltage of the FSR voltage divider.

Statistical Analysis: Pressure and flow rate data collected in this work comprised of, at minimum, a sample size of 3 (i.e., three separate devices of the same configuration). Noise in the pressure data due to the precision of the pressure sensors (small, ≈ 0.0429 psi) used was smoothed by calculating a moving average over 5 adjacent data points in time ($\Delta t \approx 0.143$ s).

Supporting Information

Supporting Information is available from the Wiley Online Library or from the author.

Acknowledgements

The authors acknowledge the University of Texas at Austin Energy Institute for funding this research.

Conflict of Interest

The authors declare no conflict of interest.

Author of Contributions

W.S. conceived the research and designed the experiments; W.S., A.D., and T.U. performed the research and acquired the data; W.S., A.D., and T.U. analyzed the data; W.S., A.D., and T.U. wrote the manuscript; W.S. and A.D. revised the manuscript; and W.S. secured the funding for this research.

Data Availability Statement

The data that support the findings of this study are available in the supplementary material of this article.

Keywords

energy storage, multifunctional, reconfigurable, soft materials

Received: January 17, 2022

Revised: March 16, 2022

Published online:

- [1] J. D. Marth, *Nat. Cell Biol.* **2008**, 10, 1015.
- [2] T. A. Campbell, S. Tibbits, B. Garrett, *Sci. Am.* **2014**, 311, 60.
- [3] G. M. Whitesides, B. Grzybowski, *Science* **2002**, 295, 2418.
- [4] R. M. Erb, J. S. Sander, R. Grisch, A. R. Studart, *Nat. Commun.* **2013**, 4, 1712.
- [5] J. W. Boley, W. M. Van Rees, C. Lissandrello, M. N. Horenstein, R. L. Truby, A. Kotikian, J. A. Lewis, L. Mahadevan, *Proc. Natl. Acad. Sci. U. S. A.* **2019**, 116, 20856.
- [6] Y. Liu, B. Shaw, M. D. Dickey, J. Genzer, *Sci. Adv.* **2017**, 3, e1602417.
- [7] Z. Ding, C. Yuan, X. Peng, T. Wang, H. J. Qi, M. L. Dunn, *Sci. Adv.* **2017**, 3, e1602890.
- [8] A. B. Subramaniam, M. Abkarian, H. A. Stone, *Nat. Mater.* **2005**, 4, 553.
- [9] S. Sacanna, M. Korpics, K. Rodriguez, L. Colón-Meléndez, S. H. Kim, D. J. Pine, G. R. Yi, *Nat. Commun.* **2013**, 4, 2.
- [10] Y. S. Cho, G. R. Yi, J. M. Lim, S. H. Kim, V. N. Manoharan, D. J. Pine, S. M. Yang, *J. Am. Chem. Soc.* **2005**, 127, 15968.
- [11] Y. Zhang, Z. Yan, K. Nan, D. Xiao, Y. Liu, H. Luan, H. Fu, X. Wang, Q. Yang, J. Wang, W. Ren, H. Si, F. Liu, L. Yang, H. Li, J. Wang, X. Guo, H. Luo, L. Wang, Y. Huang, J. A. Rogers, *Proc. Natl. Acad. Sci. U. S. A.* **2015**, 112, 11757.
- [12] S. Janbaz, R. Hedayati, A. A. Zadpoor, *Mater. Horiz.* **2016**, 3, 536.
- [13] E. Palleau, D. Morales, M. D. Dickey, O. D. Velev, *Nat. Commun.* **2013**, 4, 2257.
- [14] Y. Wang, *Biomaterials* **2018**, 178, 663.
- [15] R. Merindol, G. Delechiave, L. Heinen, L. H. Catalani, A. Walther, *Nat. Commun.* **2019**, 10, 528.
- [16] D. H. Gracias, *Curr. Opin. Chem. Eng.* **2013**, 2, 112.
- [17] Y. Mao, K. Yu, M. S. Isakov, J. Wu, M. L. Dunn, H. J. Qi, *Sci. Rep.* **2015**, 5, 13616.
- [18] J. Wu, C. Yuan, Z. Ding, M. Isakov, Y. Mao, T. Wang, M. L. Dunn, H. J. Qi, *Sci. Rep.* **2016**, 6, 24761.
- [19] H. Y. Jiang, S. Kelch, A. Lendlein, *Adv. Mater.* **2006**, 18, 1471.

- [20] M. Q. A. Rusli, P. S. Chee, R. Arsat, K. X. Lau, P. L. Leow, *Sens. Actuators, A* **2018**, 282, 17.
- [21] V. Cacucciolo, J. Shintake, Y. Kuwajima, S. Maeda, D. Floreano, H. Shea, *Nature* **2019**, 572, 516.
- [22] Q. He, S. Cai, *Sci. Rob.* **2021**, 6, 6640.
- [23] S. Li, D. M. Vogt, D. Rus, R. J. Wood, *Proc. Natl. Acad. Sci. USA* **2017**, 114, 13132.
- [24] S. M. Mirvakili, D. Sim, I. W. Hunter, R. Langer, *Sci. Rob.* **2020**, 5, 4239.
- [25] Y. Nakabo, T. Mukai, K. Asaka, *In Smart Materials III*, International Society for Optics and Photonics, Sydney, Australia **2004**, p. 132.
- [26] C. Tawk, M. in het Panhuis, G. M. Spinks, G. Alici, *Soft Rob.* **2018**, 5, 685.
- [27] G.-Y. Gu, J. Zhu, L.-M. Zhu, X. Zhu, *Bioinspir. Biomim.* **2017**, 12, 011003.
- [28] U. Gupta, L. Qin, Y. Wang, H. Godaba, J. Zhu, *Smart Mater. Struct.* **2019**, 28, 103002.
- [29] D. J. Preston, H. J. Jiang, V. Sanchez, P. Rothmund, J. Rawson, M. P. Nemitz, W. K. Lee, Z. Suo, C. J. Walsh, G. M. Whitesides, *Sci. Rob.* **2019**, 4, 1820672116.
- [30] D. J. Preston, P. Rothmund, H. J. Jiang, M. P. Nemitz, J. Rawson, Z. Suo, G. M. Whitesides, *Proc. Natl. Acad. Sci. USA* **2019**, 116, 7750.
- [31] S. Miyashita, L. Meeker, M. Go, Y. Kawahara, D. Rus, *In 2014 IEEE International Conference on Robotics and Automation (ICRA)*, IEEE, Hong Kong **2014**, p. 1446.
- [32] S. Song, S. Joshi, J. Paik, *Adv. Sci.* **2021**, 8, 2100924.
- [33] P. Rothmund, A. Ainla, L. Belding, D. J. Preston, S. Kurihara, Z. Suo, G. M. Whitesides, *Sci. Rob.* **2018**, 3, eaar7986.
- [34] B. Mosadegh, P. Polygerinos, C. Keplinger, S. Wennstedt, R. F. Shepherd, U. Gupta, J. Shim, K. Bertoldi, C. J. Walsh, G. M. Whitesides, *Adv. Funct. Mater.* **2014**, 24, 2163.
- [35] M. Wehner, R. L. Truby, D. J. Fitzgerald, B. Mosadegh, G. M. Whitesides, J. A. Lewis, R. J. Wood, *Nature* **2016**, 536, 451.
- [36] A. T. Bazin, *N. Engl. J. Med.* **1929**, 200, 442.
- [37] A. W. Caitlin, US Patent 2642259 **1953**.
- [38] A. Packard, *Nature* **1969**, 221, 875.
- [39] Y. Ding, et al., in *Storing Energy: With Special Reference to Renewable Energy Sources*, Elsevier Inc, **2016**, pp. 167–181.